International Conference on Computational Methods in Marine Engineering
MARINE 2011
L.Eça, E. Oñate, J. García, T. Kvamsdal and P. Bergan (Eds)

A NUMERICAL AND EXPERIMENTAL STUDY ON THE HYDRODYNAMIC OF A CATAMARAN VARYING THE DEMIHULL SEPARATION

S. ZAGHI*, R. BROGLIA* and A. DI MASCIO*

*Dept. of Computational Hydrodynamics at CNR-INSEAN, The Italian Ship Model Basin, via di Vallerano 128, 00139 Rome, Italy
e-mail: s.zaghi@insean.it, r.broglia@insean.it, a.dimascio@insean.it

Key words: Catamaran, Interference Effect, RANS, CFD, Towing Tests

Abstract. A complementary experimental and numerical study of the interference effect for a fast catamaran is presented. Resistance, sinkage and trim are collected by towing tank experiments for Froude number in the range from 0.2 to 0.8 for several separation distances and for the monohull. Resistance coefficient curves reveal the presence of two humps, the second one strongly depending on the separation length; high interference is observed in correspondence of the second hump. To gain a deeper insight into these behaviors, a complementary analysis is carried out by a numerical campaign; simulations are performed by means of an in-house unsteady RANS solver. Verification of numerical results is provided, together with validation, which is made by the comparison with both present and other experimental data. Agreement in terms of resistance coefficient is rather good, comparison error being always smaller than 2.2%.

1 INTRODUCTION

Both commercial and military interest is focusing on high speed multihull vessels because of their excellent performances with respect to speed, safety, resistance and transversal stability, growing up the number of studies concerging them.

The non linear interaction between the hulls makes the hydrodynamic features of a multihull vessel quite different from the one typical of monohulls. A lot of theoretical, experimental and numerical studies [1, 2, 3, 4, 5, 6, 7] have been carried out in recent years. The present study is focused on the analysis of the calm water characteristics of a fast catamaran when varying the distance between the twin hulls. The geometry considered is a high-speed catamaran designed and tested experimentally at the Technical University of Delft (Delft model 372, [8, 9]). The study is carried out by means of both towing tank experiments and computational fluid dynamics simulations. Experimental tests were conducted in the towing tank at the *Istituto Nazionale per Studi ed Esperienze*

di Archettettura Navale (CNR-INSEAN), while the numerical simulations were performed using the Unsteady Reynolds Averaged Navier Stokes Equation solver $\chi navis$, developed at CNR-INSEAN [10, 11, 12, 13].

2 EXPERIMENTAL RESULTS

The experimental campaign has been conducted in the CNR-INSEAN towing tank number 1, whose main dimensions are: $470m \times 13.5m \times 6.5m$, in length, wide and depth, respectively. The main characteristics of the set up is given here, a detailed description of the experiments (as well as the collection of all the measurements) can be found in [1]. The model is attached to the carriage-platform and it is free to pitch and heave, while the yaw motion is prevented; for the tests of the monohull, a special setup has been built to prevent roll motion too. Calm water tests were carried out at Froude numbers ranging from 0.20 to 0.80 (with a step of 0.05), for the five different demihull separations and the monohull. Repeatability tests (minimum 10 repeated tests) are provided for three Froude numbers (0.50, 0.60 and 0.75), two separation lengths ($H/Lpp = 0.167$ and 0.233) and for the monohull. These values of the Froude number were chosen on the basis of the observation that, from resistance and sea keeping tests performed at TU-Delft [8, 9], a maximum for the resistance coefficient is expected for $Fr = 0.50$; whereas $Fr = 0.60$ and 0.75 are the speeds at which maximum response for heave and pitch motions are expected.

Table 1: Model main dimensions.

Main Features	Symbol	Value
Length over all	L_{OA}	$3.11m$
Length between perpendiculars	L_{pp}	$3.00m$
Beam overall	B	$0.94m$
Beam demihull	b	$0.24m$
Demihull separation	H	$0.70m$
Drought	T	$0.15m$
Surface at rest	S	$1.945m^2$
Displacement	Δ	$87.07kg$
Vertical center of gravity	KG	$0.34m$
Longitudinal center of gravity	LCG	$1.41m$
Pitch radius of gyration	k_{yy}	$0.782m$
Moment of inertia for pitch	I_{55}	$53.245kg\,m^2$
Block coefficient	C_B/T	0.403

A geosym model of the DELFT-372 catamaran has been built in fiber glass; the main characteristics are given in table 1, whereas the geometry is shown in figure 1.

To perform an experimental analysis of the separation length effects, a mechanism which allows to change the distances between the demihull has been built; five different separations were considered: starting from the nominal one, which is $H = 0.70m$ ($H/L_{pp} = 0.233$), two wider configurations ($H = 0.80m$, $0.90m$, i.e. $H/L_{pp} = 0.267$, 0.300) and two narrower ($H = 0.60m$, 0.50, i.e. $H/L_{pp} = 0.200$, 0.167) have been considered. It has to be noted that by means of an estimation based on the Kelvin angle, even for the largest separation the interaction between the bow waves occurs. Tests have been also carried out for the monohull, the evaluation of the

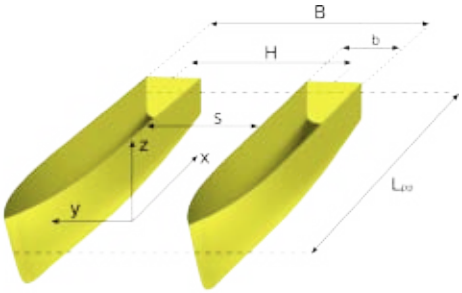

Figure 1: Model geometry

resistance interference being the main scope of the paper.

In figure 2 the total resistance coefficient versus Froude number are shown for five configurations and for the monohull (resistance for the monohull is doubled). The resistance coefficient is defined as $C_T = R_T/(0.5\rho U_\infty^2 S)$, where R_T is the dimensional resistance, ρ is density of the water, U_∞ is the undisturbed velocity and S is the wet surface at rest. The resistance and the resistance coefficient are corrected to the standard temperature of 15^o following the ITTC procedure.

For low speed, the resistance coefficient seems to be independent on the separation length, the differences between the measurements for catamarans and the monohull being negligible. Around $Fr = 0.40$, a rather large increase in the slope of the resistance can be seen for the catamaran, and its value becomes larger than twice the resistance of the monohull at the same speed, i.e. an unfavorable interference is experienced. Moreover the resistance increases when reducing the separation. At higher Froude number, the increase of the resistance coefficient with the speed for the catamaran is smaller than for the monohull; as a consequence from $Fr = 0.75$ the difference between the catamarans and the monohull becomes negligible, for all the configurations but the narrowest one.

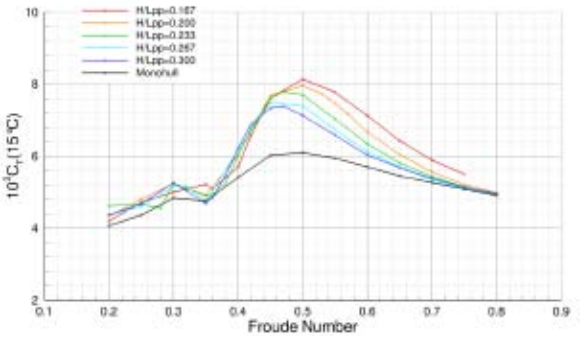

Figure 2: Total resistance coefficient versus speed

A weak slope variation on the resistance coefficient curve at low Froude number (around $Fr = 0.30$) can also be seen. The C_T curve shows the presence of two humps. This trend and the presence of regions with large slope variation is rather classical for multihull vessels, see for example [4, 6, 14]. These two humps (as the following analysis of the flow field will confirm) are related with the position and the depth of the waves crests and troughs in the inner and outer region. A clear dependence on the separation length can be inferred for the maximum value of the resistance coefficient attained at the second hump; as the separation distance decreases the maximum value for C_T increases, and is reached at increasing Froude number. In this speed range, the augmented resistance experienced by the catamaran is mostly due to an increase in the wave resistance. During the experiments also the attitude of the model has been measured. The whole experimental data can be found in [15, 16, 17].

Repeatability tests (minimum 10 repeated tests) are provided for three values of the Froude number (namely, 0.50, 0.60 and 0.75) and two separation lengths ($H/L_{pp} = 0.167$ and 0.233) as well as for the monohull; results are summarized in Table 2, where the precision indexes for sinkage, trim and total resistance coefficient are reported in percent. The precision index of the sample mean has been computed as $PI = \frac{t \cdot S}{\sqrt{N}}$ where t is equal to 2.0,

$S = \sqrt{\frac{\sum_{i=1}^{N}(x_i - \bar{x})}{N-1}}$ is the standard deviation for the N repeated samples. In order to avoid unreasonable numbers when the measured value tends to zero, the values are referred to maximum measured value.

In general, the analysis reveals a rather good repeatability for the experimental measurements of both resistance coefficient and trim; higher uncertainty is found for the measurements of the sinkage. Repeatability seems to be independent on both the speed of advancement and the distance between the hulls, whereas higher uncertainty is clearly observed for the monohull.

Table 2: Precision indexes summary.

		$H/L_{pp} = 0.167$	$H/L_{pp} = 0.233$	Monohull
Sinkage	$Fr = 0.50$	2.04%	2.91%	6.01%
	$Fr = 0.60$	2.63%	3.41%	2.81%
	$Fr = 0.75$	1.31%	2.47%	5.53%
Trim	$Fr = 0.50$	0.70%	1.30%	1.59%
	$Fr = 0.60$	0.63%	1.25%	0.62%
	$Fr = 0.75$	0.75%	1.23%	1.01%
$C_T(15°)$	$Fr = 0.50$	0.11%	0.21%	0.09%
	$Fr = 0.60$	0.09%	0.19%	0.06%
	$Fr = 0.75$	0.19%	0.13%	0.09%

When comparing the total resistance (or the total resistance coefficients) for the catamaran and the monohull (see figure 2), it is evident that, for a wide range of speed, the drag experienced by the catamaran is larger than twice the corresponding value for the monohull, the augmented resistance being to be attributed to the interference between the twin hulls. Its measure can be obtained from the interference factor defined as $I_F = \frac{C_T^{(C)} - C_T^{(M)}}{C_T^{(M)}} = \frac{R_T^{(C)} - 2R_T^{(M)}}{2R_T^{(M)}}$ having denoted with M and C quantities concerning the monohull and the catamaran, respectively. Positive and negative interference correspond to situation where the interference between the twin hulls leads to a resistance increase (unfavorable interference) or decrease (favorable interference).

Figure 3 shows the behavior of the interference factor for the separations considered as a function of the Froude number. For values up to 0.30 the interference is small and positive, i.e. there are no relevant separation length effects. When increasing the speed, a region with zero or even negative interference appears; around $Fr = 0.35$ favorable interference can be observed for the larger separations (i.e. for $H/L_{pp} = 0.267,\ 0.300$). In this region, a fairly significant interference effect is seen; indeed, I_F increases with the gap between the twin hulls. This negligible or favorable interference region clearly corresponds to the local minimum in the resistance coefficient shown in figure 2 and it is attained when a wave crest in the inner region is at the stern. It has to be noted that from the nominal separation to the smallest one the interference is positive for every Froude, i.e. for these configurations no favorable

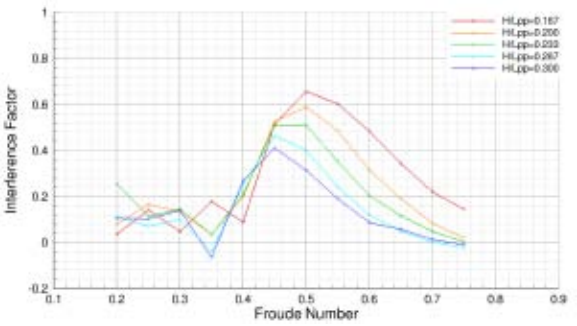

Figure 3: Interference factor.

interference is observed; the tendency to develop favorable interference region for the larger separations has been also observed in [6]. Figure 3 also highlights that for all the separations there is a maximum positive interference between $Fr = 0.45$ and $Fr = 0.50$, depending on the H/L_{pp} ratio; the maximum value attained and the speed at which it is reached depend on the distances between the hull: as the separation decreases, the maximum value for the interference factor increases, i.e. the interference between the twin hulls causes a non linear increase of the resistance; moreover, the maximum value is attained at higher speed as the gap narrows. As expected, at high Froude numbers ($Fr = 0.75$), a negligible interference is observed for all the demihull separations but the narrowest, for which, as already said, the resistance can be affected by the wave impact on the transversal beam.

An accurate analysis of the wave and the flow fields at speeds where possible favorable interference (i.e. $Fr = 0.30$), high interference ($Fr = 0.50$) and zero interference ($Fr = 0.75$) occur, will be performed by means of numerical simulations in the following sections.

3 NUMERICAL RESULTS

The numerical simulations have been done by a code (χnavis) developed at CNR-INSEAN based on the Unsteady RANS Equations. The numerical model is based on finite volume formulation with conservative variables co-located at cell centred. The spatial discretization of the convective terms is done with second order ENO-type scheme. The diffusive terms are discretized with second order centred scheme. The time integration is done by second order implicit scheme (three points backward); the solution at each time step is done by pseudo-time integration by means of Euler implicit scheme with approximate factorization with local pseudo time step and multi-grid acceleration. The turbulent viscosity has been calculated by means of the one–equation model of Spalart and Allmaras. Free surface effects are taken into account by a single phase level-set algorithm. Complex geometries and multiple bodies in relative motion are handled by a dynamical overlapping grid approach. High performance computing is achieved by an efficient shared and distributed memory parallelization. For more details on the numerical code used the interested reader is referred to [13, 10, 11, 12, 18].

The numerical analysis is carried out for three values of the Froude number, namely $Fr = 0.30$, 0.50 and 0.75. In order to analyze the effect of the demihull separations the simulations are performed for three values of the ratio H/L_{pp}, namely $H/L_{pp} = 0.167$, 0.200 and 0.233; numerical computations for the monohull have also been carried out at the same velocities. The attitudes for both the catamaran and the monohull are fixed at the dynamical positions taken from the measurements reported in the previews section. The numerical solutions were computed by means of a Full Multi Grid-Full Approximation Scheme (FMG-FAS), with four grid levels, each obtained from the next finer by removing every other grid points; the three finest grids (for which the refinement ratio is 2) have been used for Verification and Validation purposes.

The computational domain is discretized by means of an overlapped multiblock grid.

The mesh around the catamaran consists of about 9.5 million cells distributed in 55 patched and overlapped blocks; for the grid around the monohull a total of about 4.3 million volumes are distributed in 32 blocks. Due to the symmetry about the vertical plane, for the catamaran only one hull is discretized, whereas for the monohull only half hull is considered; in both cases, symmetry boundary conditions are enforced on the plane $y = 0$. Overlapping grids capabilities are exploited to attain high quality meshes and for refinement purposes.

3.1 Verification and validation

Verification and validation have been carried out for the total resistance coefficient. The analysis has been carried out for all the numerical simulations. Results are summarized in table 3. Since negligible iterative uncertainty has been observed (well below 1%), grid uncertainty can be considered as the only contribution to the numerical uncertainty.

Table 3: Verification & Validation for C_T.

H/L_{pp}	Fr	S_3	S_2	S_1	P_{RE}	δ_{RE}	S_{RE}	$\frac{P_{RE}}{P_{Th(2)}}$	$\frac{U_{FS}}{S_{RE}}\%$	Err. %
0.167	0.30	$5.64\,10^{-3}$	$5.19\,10^{-3}$	$5.06\,10^{-3}$	1.825	$5.02\,10^{-5}$	$5.01\,10^{-3}$	0.912	1.678	0.080
	0.50	$8.66\,10^{-3}$	$8.21\,10^{-3}$	$8.12\,10^{-3}$	2.378	$2.06\,10^{-5}$	$8.10\,10^{-3}$	1.189	1.197	0.728
	0.75	$5.91\,10^{-3}$	$5.51\,10^{-3}$	$5.42\,10^{-3}$	2.281	$2.16\,10^{-5}$	$5.40\,10^{-3}$	1.141	1.561	2.064
0.233	0.30	$5.53\,10^{-3}$	$5.22\,10^{-3}$	$5.26\,10^{-3}$	Oscillatory	$\diagdown$	$\diagdown$	$\diagdown$	$\diagdown$	0.100
	0.50	$8.15\,10^{-3}$	$7.79\,10^{-3}$	$7.70\,10^{-3}$	1.906	$3.45\,10^{-5}$	$7.66\,10^{-3}$	0.953	0.738	0.714
	0.75	$5.75\,10^{-3}$	$5.30\,10^{-3}$	$5.16\,10^{-3}$	1.680	$6.36\,10^{-5}$	$5.10\,10^{-3}$	0.840	2.167	1.142
0.300	0.30	$5.54\,10^{-3}$	$5.22\,10^{-3}$	$5.30\,10^{-3}$	Oscillatory	$\diagdown$	$\diagdown$	$\diagdown$	$\diagdown$	0.552
	0.50	$7.64\,10^{-3}$	$7.24\,10^{-3}$	$7.14\,10^{-3}$	2.013	$3.29\,10^{-5}$	$7.11\,10^{-3}$	1.006	0.788	0.550
	0.75	$5.74\,10^{-3}$	$5.25\,10^{-3}$	$5.14\,10^{-3}$	2.141	$3.27\,10^{-5}$	$5.10\,10^{-3}$	1.071	1.767	0.926
Monohull	0.30	$2.62\,10^{-3}$	$2.50\,10^{-3}$	$2.44\,10^{-3}$	0.953	$6.76\,10^{-5}$	$2.37\,10^{-3}$	0.476	5.833	2.245
	0.50	$3.39\,10^{-3}$	$3.19\,10^{-3}$	$3.13\,10^{-3}$	1.888	$2.05\,10^{-5}$	$3.11\,10^{-3}$	0.944	1.083	1.949
	0.75	$2.88\,10^{-3}$	$2.68\,10^{-3}$	$2.60\,10^{-3}$	1.433	$4.50\,10^{-5}$	$2.55\,10^{-3}$	0.717	3.242	0.164

The values S_3, S_2 and S_1 are the total resistance coefficients computed on the coarse, the medium and the fine grid, respectively; $p_{RE} = \frac{ln(\varepsilon_{32}/\varepsilon_{21})}{ln(r)}$ is the order of accuracy, where $\varepsilon_{21} = S_2 - S_1$, $\varepsilon_{32} = S_3 - S_2$ and r is the grid refinement ratio ($r = 2$ in the current analysis). From the solution on the medium and the finest grid, the Richardson's Extrapolated error can be computed as $\delta_{RE} = \frac{\varepsilon_{21}}{r^{p_{RE}}-1}$. The generalized Richardson Extrapolated solution S_{RE} can be then estimated as $S_{RE} = S_1 - \delta_{RE}$. When monotonic convergence is attained (i.e. $0 < \varepsilon_{21}/\varepsilon_{32} < 1$) both the order of convergence and the error can be computed. In the present work the factor of safety method proposed by [19] has been adopted. The error with respect the experiment data is reported in the last column of the table 3 in percentage of the experimental data D: $err = \frac{S_{RE}-D}{D}\%$.

All the simulations show monotonic convergence except the simulations at $Fr = 0.30$ with separations ratios $H/L_{pp} = 0.233, 0.300$, for which an oscillatory convergence is observed. In this case the Richardson's Extrapolated error is not computed, and the comparison is made with the numerical solution on the finest grid. Generally the observed order of convergence is close to the theoretical value for all the cases where monotonic convergence is attained and very low uncertainties are estimated for all monotonic convergent cases. By comparison with the experimental data, a very good agreement between numerical results and experimental measurements can be inferred: the largest error is about 2% and it is observed for monohull computations (at $Fr = 0.30, 0.50$) and for the

narrowest separation at $Fr = 0.75$. Where the monotonic convergence is achieved the numerical results can be considered validated.

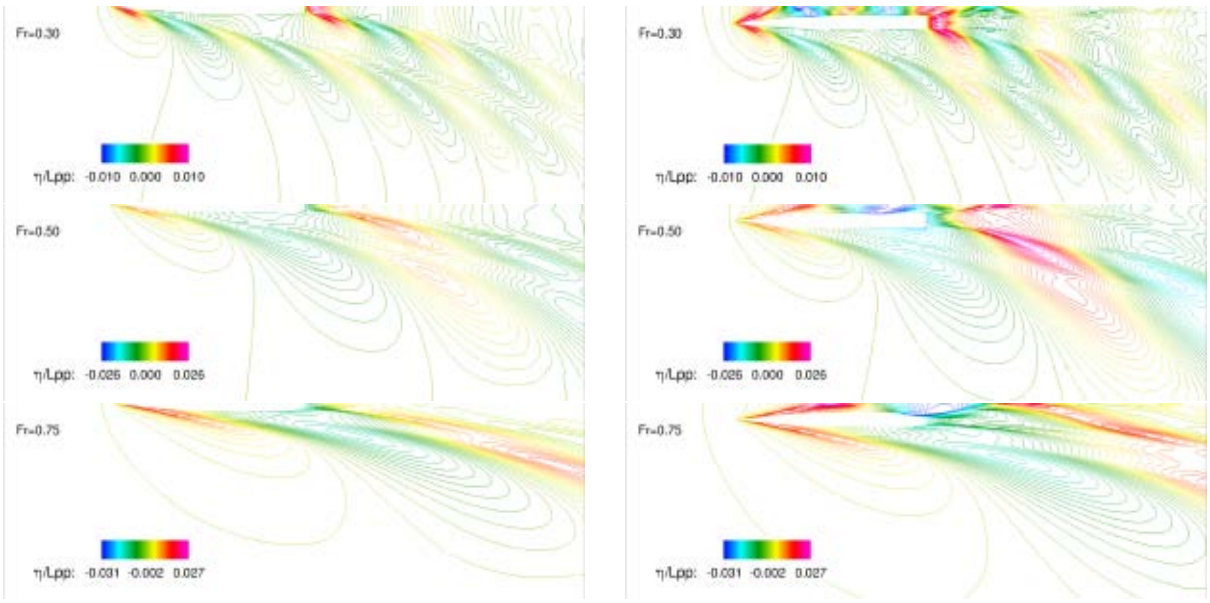

Figure 4: Wave patterns: monohull (left) and catamaran with separation length $H/Lpp = 0.167$ (right)

3.2 Wave patterns and wave cuts analysis

Figures 4÷5 show the computed wave patterns for both the catamaran and the monohull. Comparing the monohull and the catamaran, as well as among those for the catamaran at different separation lengths, the external wave pattern is always slightly influenced by the presence of the twin hull, at least up to the aft perpendicular. On the contrary, strongly interference effects is seen in the whole inner region. The interaction between the transversal bow wave systems generates a deep trough. At low Froude number, due to the interaction of the second waves (that looks like a reflection from the symmetry plane in the simulations reported) a second wave trough is present in the inner region; the magnitude is smaller then the previous one. The resistance coefficient (see figure 2) is strongly influenced by this waves system; the first hump of the resistance coefficient occurs when the second wave trough overtakes the stern, whereas the second hump is due to the passage of the first trough. As the Froude number increases, the resistance coefficient increases until the the wave trough overtakes the stern; after that, the resistance coefficient decreases. The maximum value for the resistance coefficient is attained when the first trough (the deeper) is at the stern (see also [1, 14]). The inner wave crest and trough move downstream as the separation distance increases for fixed Froude number. This also implies that the first trough will reach the stern at higher speed as the separa-

tion decreases. As a consequence, the speed at which the maximum value for the total resistance coefficient is attained increases as the separation distance decreases.

The wave patterns also highlights a strong interference between the stern wave systems; for all the separations and the speeds computed, the catamaran shows a much higher rooster tail than the monohull.

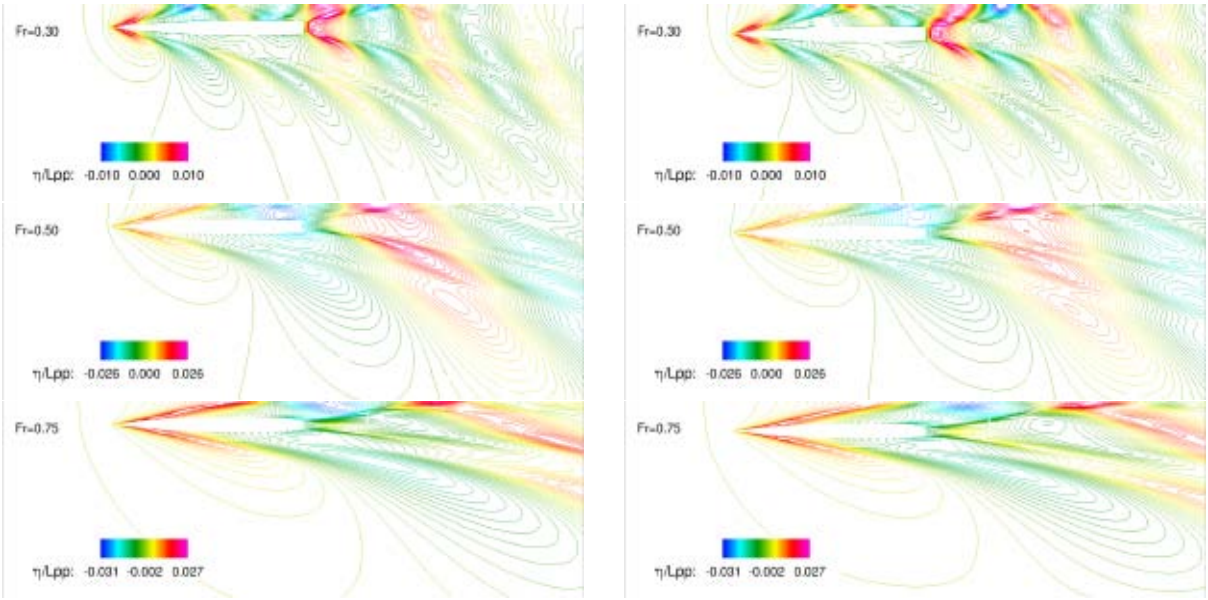

Figure 5: Wave patterns: catamaran with separation length $H/Lpp = 0.233$ (left) and catamaran with separation length $H/Lpp = 0.300$ (right)

Figure 6a) shows the longitudinal wave cuts in the outer region (at distance $y = s/2$ from the side of the hull); the wave cuts are compared with those of the monohull at an equivalent distance for the analysis of the wave interference. This comparison confirm the weak influence of the interference between the hulls in the outer region, the larger differences between the catamaran and the monohull being located around and downstream the aft perpendicular (AP). Differences behind the stern are clearly due to the interference phenomena between the waves generated at the stern, whereas, for those around the aft perpendicular it is not clear if these differences should be ascribed to the difference in trim or to the interference between the hulls (see also [6]). To clarify this point, a numerical simulation of the monohull at the same attitude of the catamaran with the narrowest separation length at $Fr = 0.50$ has been performed; the obtained wave cut is reported with black line in the top picture of figure 6a. As it can be seen, the variation in trim has an effect in the hollow and the rooster tail only, i.e. the difference in wave cuts at the transom is due mainly to the interference between the two hulls. This indicates that to achieve a correct analysis of the wave interference, monohull wave cuts should be used rather than the outer wave cuts of the catamaran.

Figure 6b) presents a comparison between the longitudinal wave cuts along the catamaran center plane with twice those of the monohull at an equivalent distance. For the largest separation ($H/L_{pp} = 0.300$) the differences between mono and multi hulls wave elevations are rather small, confirming that the interference factor (see also figure 3) is small. Differences increase as the distance between the hulls decreases; for both the nominal and the narrowest separations, larger differences are observable at medium speed, i.e. when maximum interference occurs. It is interesting to note that at $Fr = 0.30$ the wave cuts (between FP and AP) for the catamaran is generally higher than twice of the monohull (i.e. significant unfavorable interference) only for the narrowest separation. This again confirms what observed in the discussion of the interference factor, where clear unfavorable interference around $Fr = 0.30$ has been observed only for $H/L_{pp} = 0.167$.

The complete analysis of the numerical simulations can be found in [17].

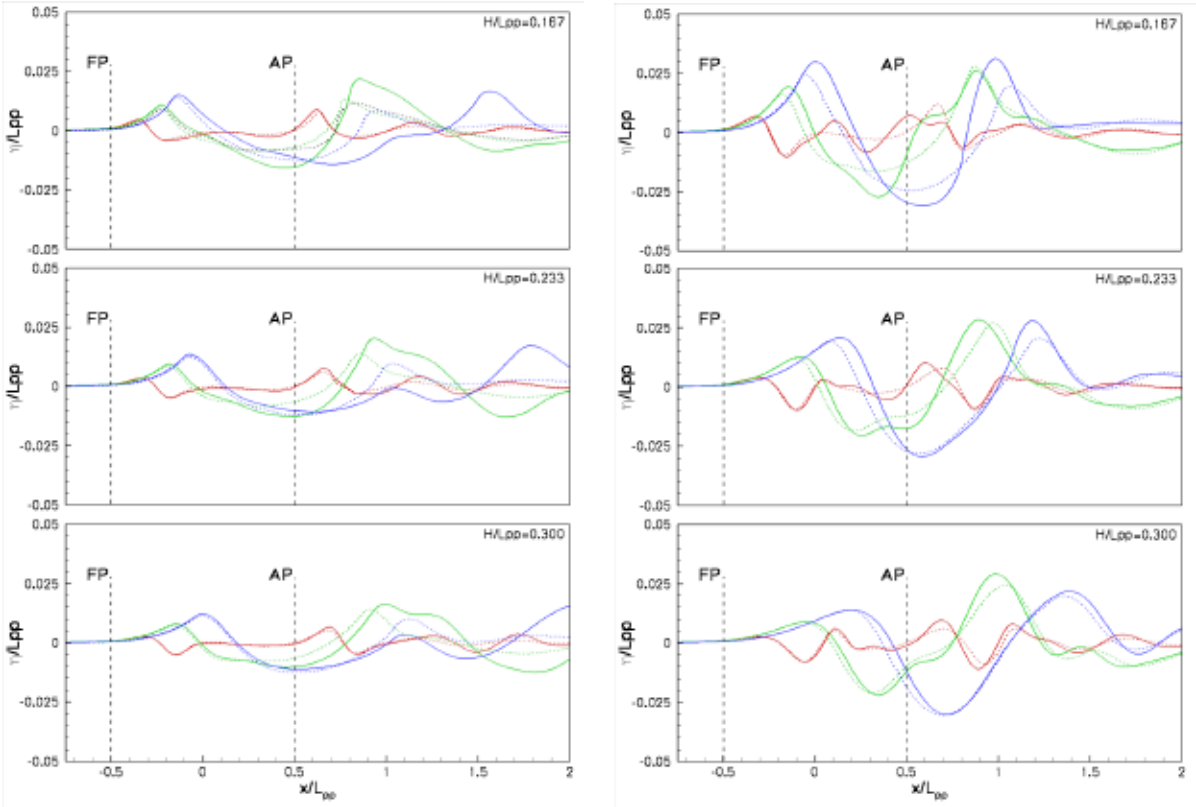

(a) Longitudinal wave cuts at distance $y/s = 1/2$ from the side of the hull in the outer region: red $Fr = 0.30$, green $Fr = 0.50$ and blue $Fr = 0.75$; catamaran in solid line, monohull in dotted line.

(b) Longitudinal wave cuts along the centerline at an equivalence distance for the monohull. Wave cuts for the monohull are doubled; legend as in the previous figure.

Figure 6: Waves elevation comparison

4 CONCLUSIONS

It has been presented the ongoing experimental and numerical investigations on the high-speed catamarans demi-hulls interference effects done at the CNR-INSEAN facilities. The effects of the separation distances between the hulls is the focus of this study. Resistance, trim and sinkage have been experimentally measured for several demihull separations in the CNR-INSEAN towing tank, highlighting the presence of two humps in the resistance coefficient curve. The separation distance clearly influence the second hump; indeed, maximum resistance coefficient increases as the sepration length decreases, and it occurs at higher speed. Computing the interference factor, the local maximum interference has been observed in correspondence of the two humps in the resistance coefficient curve. A region of possible favorable interference (i.e. a local minimum for the interference factor) has been observed for a Froude number around 0.35 with near-negative interference for the wider separation distances. The maximum value for the interference takes place for Froude number around 0.50; the value increases and occurs at higher speeds as the gap between the two hull decreases. Negligible interference has been observed at very high speeds (higher than 0.75).

Numerical simulations have been undertaken using a code developed at INSEAN-CNR, which is a finite volume second order accurate solver for the unsteady incompressible Navier Stokes equations. Numerical simulations were performed for $Fr = 0.30$, 0.50 and 0.75, and for the nominal, the narrowest and the widest separation distances and for the monohull. The wave field has been related with the resistance coefficient curve, as well as with the interference highlighting the influence of wave troughs on the C_T behaviour.

Acknowledgments

This work has been done in the framework of an ongoing NICOP collaboration project between CNR-INSEAN and The Iowa Institute of Hydraulic Research (IIHR), for which activities include experimental tests in both calm water and in waves, as well as complementary numerical simulations.

The activities reported here have been financially supported by the U.S. Office of Naval research, through Dr. L. Patrick Purtell in the framework of the NICOP project *"Complementary EFD and CFD Analysis of Calm Water Hydrodynamics and Large Amplitude Motion for High-Speed Catamarans"*, grant N00014-08-1-1037. Numerical computations presented here have been performed on the parallel machines of CASPUR Supercomputing Center (Rome); their support is gratefully acknowledged. The authors wish to thank Prof. F. Stern for his suggestions and helpful discussions which have contributed to this work.

REFERENCES

[1] R. Broglia, S. Zaghi, and A. Di Mascio. Numerical Simulation of Interference Effects for a High-Speed Catamaran *submitted to Journal of Marine Science and Technology*,

2011.

[2] L.J. Doctors. The Influence of Viscosity on the Wavemaking of a Model Catamaran In 8^{th} *International Workshop on Water Waves and Floating Bodies, Le Croisic, France*, pages 12–1, 2003.

[3] M. Insel and AF Molland. Investigation into the resistance components of high speed displacement catamarans. *Transactions of Royal Institute of Naval Architects*, pages 1–20, 1992.

[4] A. Millward. The effect of hull separation and restricted water depth on catamaran resistance *Transactions of Royal Institute of Naval Architects*, 134:341–349, 1992.

[5] AF Molland, PA Wilson, DJ Taunton, S. Chandraprabha, and PA Ghani. Resistance and wash measurements on a series of high speed displacement monohull and catamaran forms in shallow water. *International Journal of Maritime Engineering*, 146(2):19–38, 2004.

[6] A. Souto-Iglesias, R. Zamora-Rodríguez, D. Fernández-Gutiérrez, and L. Perez-Rojas. Analysis of the wave system of a catamaran for CFD validation *Experiments in Fluids*, 42(2):321–332, 2007.

[7] S. Zaghi, R. Broglia, and A. Di Mascio. Experimental and numerical investigations on fast catamarans interference effects *Journal of Hydrodynamics, Ser. B*, 22(5):545–549, 2010.

[8] R. van't Veer. Experimental results of motions and structural loads on the 372 catamaran model in head and oblique waves Technical report, TU Delft, Report N.1130, 1998.

[9] R. van't Veer. Experimental results of motions, hydrodynamic coefficients and wave loads on the 372 Catamaran model Technical report, TU Delft, Report N.1129, 1998.

[10] A. Di Mascio, R. Broglia, and B. Favini. A second order Godunov-type scheme for naval hydrodynamics In *Godunov Methods: Theory and Applications*, volume 26, pages 253–261. Kluwer Academic/Plenum Publishers, 2001.

[11] A. Di Mascio, R. Broglia, and R. Muscari. On the application of the single-phase level set method to naval hydrodynamic flows *Computers & Fluids*, 36(5):868–886, 2007.

[12] A. Di Mascio, R. Broglia, and R. Muscari. Prediction of hydrodynamic coefficients of ship hulls by high-order Godunov-type methods *Journal of Marine Science and Technology*, 14(1):19–29, 2009.

[13] R. Broglia, A. Di Mascio, and G. Amati. A Parallel Unsteady RANS Code for the Numerical Simulations of Free Surface Flows In 2^{nd} *International Conference on Marine Research and Trasportation, Ischia, Naples, Italy*, 2007.

[14] F. Stern, P. Carrica, M. Kandasamy, J. Gorski, J. O'Dea, M. Hughes, R. Miller, D. Hendrix, D. Kring, W. Milewski, et al. Computational hydrodynamic tools for high-speed sealift *SNAME Transactions*, 114:55–81, 2006.

[15] R. Broglia, S. Zaghi, B. Jacob, A. Olivieri, and A. Iafrati. Wave cuts for the INSEAN-2554 catamaran model at several hull separations. Technical Report in preparation, CNR-INSEAN, Istituto Nazionale per Studi ed Esperienze di Architettura Navale, 2011.

[16] R. Broglia, S. Zaghi, and F. Stern. Calm water tests for the INSEAN-2554 catamaran model at several hull separations. Technical Report in preparation, CNR-INSEAN, Istituto Nazionale per Studi ed Esperienze di Architettura Navale, 2011.

[17] S. Zaghi, R. Broglia, and A. Di Mascio. Analysis of the Interference Effects for High-Speed Catamarans by Model Tests and Numerical Simulations *submitted to Ocean Engineering*, 2011.

[18] R. Muscari, R. Broglia, and A. Di Mascio. An overlapping grids approach for moving bodies problems In 16^{th} *International Offshore and Offshore and Polar Engineering Conference Proceedings*. ISOPE, Cupertino, CA, 95015-0189, USA, 2006.

[19] T. Xing and F. Stern. Factors of Safety for Richardson Extrapolation *Journal of Fluids Engineering*, 132:061403–1, 2010.